frontiers | Frontiers in Virology

TYPE Brief Research Report
PUBLISHED 03 February 2025
DOI 10.3389/fviro.2025.1547176

OPEN ACCESS

EDITED BY
Tsutomu Murakami,
National Institute of Infectious Diseases (NIID), Japan

REVIEWED BY
Akatsuki Saito,
University of Miyazaki, Japan
Kazuaki Monde,
Kumamoto University, Japan

*CORRESPONDENCE
Lionel Berthoux
lionel.berthoux@uqtr.ca

RECEIVED 17 December 2024
ACCEPTED 15 January 2025
PUBLISHED 03 February 2025

CITATION
Singh A, Fourcassié V, Gonçalves Dos Santos KC, Chelbi H, Merindol N, Droit A, Germain H and Berthoux L (2025) Effects of GS-CA1 on nuclear envelope-associated early HIV-1 infection steps. *Front. Virol.* 5:1547176. doi: 10.3389/fviro.2025.1547176

Effects of GS-CA1 on nuclear envelope-associated early HIV-1 infection steps

Amita Singh[1], Victor Fourcassié[2,3], Karen Cristine Gonçalves Dos Santos[4], Hocine Chelbi[1], Natacha Merindol[3], Arnaud Droit[2,3], Hugo Germain[4] and Lionel Berthoux[1]*

[1]Department of Medical Biology, Université du Québec à Trois-Rivières, Trois-Rivières, QC, Canada, [2]Proteomics Platform of the Centre Hospitalier Universitaire de Québec - Université Laval, Québec, QC, Canada, [3]Centre de recherche du Centre Hospitalier Universitaire de Québec - Université Laval, Québec, QC, Canada, [4]Department of Chemistry, Biochemistry and Physics, Université du Québec à Trois-Rivières, Trois-Rivières, QC, Canada

The novel HIV-1 drugs GS-CA1 and the recently approved lenacapavir (GS-6207) target the viral structural protein capsid (CA). However, their multiple mechanisms of action have not been fully characterized. Here, we investigated the effects of GS-CA1 on the early stages of HIV-1 infection, specifically the steps involving the nuclear envelope, in comparison to the antiviral cytokine IFN-β. Mass spectrometry data indicated that nuclear envelope proteins were only modestly affected by either GS-CA1 treatment or HIV-1 infection, but combining the two had a more significant impact, altering the levels of many proteins including proteasomal components. GS-CA1 induced a small but clear accumulation of HIV-1 capsid cores at nuclear pores, as seen by microscopy, whereas IFN-β caused a strong accumulation of HIV-1 cores at the nuclear envelope but not specifically at nuclear pores. These observations are consistent with GS-CA1 inhibiting the nuclear translocation of HIV-1 capsid cores through nuclear pores.

KEYWORDS

HIV-1, HIV-1 capsid, GS-CA1, mass spectrometry, nuclear pore complex, nuclear envelope, interferon

Introduction

HIV-1 capsid (CA) proteins have a central role in several early post-entry stages of infection, including retrograde transport, nuclear import and integration (1–5). In particular, CA is key to HIV-1 nuclear import through nuclear pore complexes (NPCs), which are large protein channels embedded in the nuclear envelope. Comprising multiple

copies of nucleoporins (Nups), NPCs facilitate the bidirectional transport of macromolecules such as proteins, RNA and ribonucleoprotein complexes [reviewed in (6)]. About one-third of Nups contain phenylalanine-glycine-rich motifs (FG repeats) and are important for the selection of cargos to be transported through NPCs (7). Consistent with its central role in nuclear import, CA was found to interact with several FG-containing Nups, such as Nup88, Nup214, Nup358/RanBP2 (cytoplasmic side); Nup62, Nup98, Nup107 (central ring); and Nup153 (nuclear basket) (8–10) [reviewed in (11)]. These findings have led to a model whereby the capsid core interacts sequentially with various Nups present in NPCs, driving its import to the nucleus (11). Interestingly, HIV-1 was also found to modulate the levels of Nup358 at NPCs (12, 13), which opens the possibility that HIV-1 cores affect NPCs integrity instead of simply using them to achieve passage to the nucleus. In addition to being relevant to HIV-1 nuclear import, NPCs are key to antiviral responses triggered by type I interferons (IFN-I), including IFN-β. For instance, IFN-I-induced antiviral protein Mx2 (MxB) interactions with multiple nucleoporins is required for its inhibitory activity against HIV-1 at the nuclear import step (14). Interestingly, CA is the target of Mx2, and their interaction results in a block to HIV-1 nuclear transport (15, 16). Furthermore, NPCs play a central role in the signaling cascades that form the basis of the IFN-I pathway, and as a result, viruses are known to interfere with the nuclear-cytoplasmic transport of IFN-I signaling components (17).

Current HIV pharmacological treatments rely largely on targeting the viral enzymes protease, reverse transcriptase and integrase. By contrast, GS-CA1 and the structurally close GS-6207 (lenacapavir) are CA inhibitors that disrupt viral capsid formation by interfering with CA-CA interactions (18). In clinical trials, GS-6207/lenacapavir has demonstrated efficacy against multidrug-resistant HIV-1 strains (19) and was approved in 2022 for the treatment of heavily treatment-experienced individuals (20). GS-CA1 has not been pursued in humans but showed a strong protective effect against HIV-1 in a primate model (21). Consistent with the important role for CA in both early and late stages of the virus life cycle, GS-CA1 and GS-6207 have pleiotropic effects on HIV-1 (18, 22, 23). Their effects on early stages seem to stem from a stabilization of the viral capsid core, as seen in "fate-of-capsid assays" (22, 24). Quantitative analyses of reverse transcribed HIV-1 cDNA as well as its specifically nuclear species (2-LTR DNA and integrated DNA) suggest that GS-CA1 and GS-6207 can inhibit several early HIV-1 replication steps, including nuclear import (18, 22, 23). However, discordant results were obtained from another team, who did not observe an effect of GS-CA1 on CA presence in the nucleus following infection (24). Whether GS-CA1 and GS-6207 cause HIV-1 to be specifically sequestered at NPCs is unknown. The effects of these novel CA-targeting drugs and of HIV-1 on the composition of NPCs in the early stages of the virus life cycle have never been investigated by mass spectrometry (MS). Here, using MS and immunofluorescence microscopy, we evaluated the impact of HIV-1 infection and GS-CA1 treatment, in comparison to IFN-β treatment, on the nuclear envelope and the localization of HIV-1 capsid cores at the nuclear envelope and nuclear pores.

Materials and methods

Cell culture

THP-1 monocytic cells were cultured in Cytiva HyClone RPMI 1640 medium containing L-glutamine (SH3002701) supplemented with 10% Cytiva HyClone fetal bovine serum (FBS, SH3039603) and penicillin-streptomycin (Cytiva HyClone, SV30010). Crandell-Rees Feline Kidney (CRFK) cells and human embryonic kidney 293T cells (HEK293T) were maintained in high glucose Cytiva HyClone Dulbecco's Modified Eagle's Medium (DMEM) containing L-glutamine and sodium pyruvate (SH3024301) supplemented with 10% FBS and penicillin-streptomycin. All cell culture reagents were purchased through Fisher Scientific, Ottawa, Canada.

HIV-1 vector production and titration

To produce the GFP-expressing, vesicular stomatitis virus protein G (VSV-G)-pseudotyped HIV-1 vector $NL43_{GFP}$, HEK293T cells were transfected with 10 µg $pNL43_{GFP\Delta Env\Delta Nef}$ (25, 26) and 5 µg pMD2.G (26) using polyethyleneimine (PEI, Polysciences, Niles, IL) (27) for 16 h, after which the supernatants were replaced with fresh medium (26). The supernatants were collected 24 and 48 h later. Cell debris were removed by low-speed centrifugation (3,000 rpm, 10 min at room temperature), followed by filtration through 0.45 µm filters (Millipore Sigma Durapore PVDF). Virus titrations were performed by infecting CRFK cells with serial dilutions of the vector preparations. CRFK cells were fixed in Cytiva HyClone Dulbecco's phosphate buffer saline (PBS; #SH30028LS) containing 4% formaldehyde (37% solution, BioBasic, Quebec, Canada), and the percentage of infected cells was assessed by flow cytometry using a Beckman Coulter FC500 instrument. CRFK viral titers were calculated by analyzing flow cytometry results using FCS Express 6 software (*De Novo* Software).

EC_{50} determination

THP-1 cells were seeded at a density of 20,000 cells/well in 96-well plates. Cells were then treated with 2-fold serial dilutions of GS-CA1 (Gilead Sciences, Foster City, California, USA) and 2 h later were infected with $NL43_{GFP}$ (CRFK MOI = 1). 48 h later, cells were fixed in 4% formaldehyde and the percentage of GFP-positive cells was determined using flow cytometry. GS-CA1 EC_{50} was calculated using an online tool available at https://www.aatbio.com/tools/ic50-calculator (accessed 2021-02-08).

Large-scale infections and nuclear envelope purification

2 x 10^7 THP-1 cells cultured in flasks were treated or not with 2 nM GS-CA1 for 2 h and then were infected or not with $NL43_{GFP}$ using a viral dose (MOI = 2) leading to about 40% productively infected THP-1 cells, for 12 h. In a distinct experiment, cells were treated or not with 10 ng/ml IFN-β (PeproTech, Rocky Hill, NJ, USA) and were infected 12 h later with $NL43_{GFP}$ for 12 h. A small aliquot of the cells was preserved for flow cytometry analysis 36 h later. The remainder of the cells were processed for the extraction of nuclear envelope-enriched fractions using a Minute™ Nuclear Envelope Protein Extraction Kit (Invent Biotechnologies, Plymouth, MN, USA). Whole-cell lysates, cytoplasmic extracts, and nuclear extracts also prepared using the same kit were included in the purification validation experiments.

Western blotting

Protein concentrations in the nuclear envelope extracts were determined using the Bio-Rad Protein Assay kit and samples were normalized accordingly prior to SDS-polyacrylamide gel electrophoresis and transfer to polyvinylidene difluoride (PVDF) or nitrocellulose membranes. Blotted proteins were analyzed using the FG repeats-specific MAb414 mouse monoclonal antibody at 1:2,000 dilution (#902907, BioLegend, San Diego, CA), followed by detection with an HRP-conjugated anti-mouse secondary antibody (#7076S, New England Biolabs, Whitby, Ontario). Detection of glyceraldehyde 3-phosphate dehydrogenase (GAPDH) using the #9484 mouse monoclonal antibody (Abcam, Toronto, ON) was used as a marker for cytosolic proteins. Blots were visualized using the Thermo Scientific SuperSignal West Femto substrate, and images were recorded using the Bio-Rad ImageLab system.

Mass spectrometry

10 µg of protein from nuclear envelope-enriched fractions were reduced using 0.2 mM dithiothreitol, alkylated using 0.8 mM iodoacetamide and digested with 0.2 µg of trypsin (sequencing grade, Promega, Madison, WI). Samples were analyzed by nano-LC/MSMS using a Dionex UltiMate 3000 nanoRSLC chromatography system (Thermo Fisher Scientific) interfaced to an Orbitrap Fusion mass spectrometer (Thermo Fisher Scientific, San Jose, CA, USA) equipped with a nanoelectrospray ion source. 1 µg of peptides were separated on a C18 Pepmap Acclaim column (50 cm length, 75 µm internal diameter) using a 90 min linear gradient at 300 nL/min with 5-40% solvent B (A: 0.1% formic acid, B: 80% acetonitrile, 0.1% formic acid). Mass spectra were obtained with a data-dependent acquisition method using the Thermo XCalibur software version 4.1.50. Full scan mass spectra (350–1800 m/z, 120,000 resolution) were acquired from Orbitrap using an AGC target of 4e5 with a maximum injection time of 50 ms. Precursors were filtered in the quadrupole analyzer with 1.6 m/z isolation windows and fragmented by higher-energy Collision-induced Dissociation (HCD) with 35% collision energy. The resulting fragments were detected using the linear ion trap at a rapid scan rate with an AGC target of 1e4 and a maximum injection time of 50 ms.

MS data analysis

For the IFN-β-treated THP-1 cells experiment, the acquired spectra were processed using the Minora feature detector algorithm in Proteome Discoverer 2.3 (Thermo Fisher Scientific). The resulting data were subjected to MASCOT searches against the UniProt *Homo sapiens* protein database (reference proteome UP000005640 with 74485 entries, downloaded on 2019-02-12) considering trypsin digestion. For protein validation, a false discovery rate (FDR) of ≤ 0.01 was allowed at peptide and protein levels based on a target/decoy search. Unique and razor peptides were considered for protein quantification, and normalization was performed based on the summed abundance of the peptides. The data were normalized using the intensity normalization factor, which was calculated by dividing the median intensity for each sample by the median intensity for all samples combined. The results were exported to an Excel file where samples were compared to each other using absolute Z-score > 1.96, q-value < 0.05 and log2 ratio between the two conditions > 0, in order to determine the statistical significance of the observed variations. For the GS-CA1 experiments, spectra were analyzed in Maxquant using the Andromeda search engine (version 2.0.2.0) against a UniProt *Homo sapiens* protein database (reference proteome UP000005640 with 97094 entries, downloaded on 2020-09-24). Trypsin was set as the digestion parameter and a maximum FDR of 1% was set both at the peptide and protein level. The proteinGroups.txt output file was imported into R software and the LFQ normalized intensities were used to compare the groups considering the same Z-score and q-value thresholds as above.

Microscopy

Cells were fixed in 4% formaldehyde and permeabilized with Triton X-100 (0.2%) in 1x PBS for 10 min. Cells were then stained for HIV-1 CA protein using a mouse monoclonal antibody (Clone 183 diluted 1:5000, AIDS Research Reagents Program, contributed by Bruce Chesebro), co-stained for nucleoporin TPR (rabbit antibody, 1:1000 dilution, Abcam #84516), and for DNA using Hoechst 33342 (Invitrogen #3570, through Fisher Scientific Canada) (28). Alexa Fluor 488 anti-mouse and 594 anti-rabbit secondary antibodies were used (1:5000 dilution, Molecular Probes). Images were acquired with a Leica TSC SP8 confocal microscope fitted with a 63×/1.40 oil objective using the optimal resolution for the wavelength (determined using the Leica software). CA signal dots were counted out of 19-20 slides for each condition (26 to 28 cells), and CA dots that co-localized with the TPR signal were counted as well (as seen by the presence of orange color), allowing us to calculate the colocalization ratio. Counting was performed blindly, from anonymized pictures and

by a student who was not involved in the "wet lab" phase of the experiment.

Results

GS-CA1 efficiently inhibits early stages of HIV-1 infection in THP-1 cells

THP-1 monocytic cells are representative of the monocyte-macrophage lineage, one of the main types of HIV-1 host cells *in vivo* (29). To assess the effects of GS-CA1 on the early steps of HIV-1 infection in these cells, we used an NL4-3-derived, VSV-G-pseudotyped HIV-1 vector expressing GFP in place of Nef (25). VSV-G pseudotyping greatly increases virus entry efficiency, allowing for detection of HIV-1 cores in cells by MS and by microscopy, and is not believed to alter post-fusion steps of the infection process (30). THP-1 cells were challenged with $NL43_{GFP}$ in the presence of multiple drug concentrations, and the percentage of GFP-positive cells was determined using flow cytometry (Figure 1A). We found that GS-CA1 strongly inhibits THP-1 infection, with an EC_{50} of approximately 0.125 nM (Figure 1A), which is consistent with previous studies (18).

Isolation of nuclear envelopes for mass spectrometry analyses

To analyze the effects of HIV-1 vector infection and/or drug treatment on nuclear pore proteins, we produced nuclear envelope-enriched fractions. First, we performed a pilot experiment with uninfected/untreated cells, to assess nuclear envelope fractions extracted using a commercial kit (Supplementary Figure S1). Whole-cell, cytoplasmic, nuclear and nuclear envelope protein lysates were obtained. "Nuclear" fractions are supernatants of the nuclear envelope precipitation step. Fractions were analyzed by Western blotting with the monoclonal antibody MAb414 which recognizes several Nups through binding to the FG repeats (31). Using this antibody, we observed an enrichment in bands above 150 kDa in the nuclear envelope fractions, consistent with the high molecular weight of several FG-containing Nups. As expected, GAPDH was absent from the nuclear envelope fractions (Supplementary Figure S1).

In the next experiment, THP-1 cells were infected or not with $NL43_{GFP}$ for 12 h, in the presence or absence of 2 nM GS-CA1, which was the lowest concentration at which no infection could be detected (Figure 1A). Quintuplicate infections were performed at a multiplicity of infection leading to about 40% infected cells in the absence of drug (Figure 1B). The GS-CA1 concentration used was 16-times higher than the observed EC_{50}. As expected, infection with the $NL43_{GFP}$ vector was completely abrogated at this concentration (Figure 1B). Nuclear envelope extracts were subjected to label-free mass spectrometry (MS). The principal component analysis (PCA) shown in Supplementary Figure S2 demonstrates that the control and GS-CA1 treated cells show only minor differences (except for sample CTRL_5), whereas the $NL43_{GFP}$-infected ("HIV-1") group and the $NL43_{GFP}$-infected + GS-CA1-treated group are clearly distinct. Supplementary Figure S3 summarizes the number of proteins quantified for each condition, as well as the number of proteins found to be regulated in pairwise analyses, showing that the greatest number of dysregulated proteins is found when comparing HIV-1 + GS-CA1 to either control samples or GS-CA1-treated ones.

Effect of HIV-1 and GS-CA1 on nuclear envelope-associated proteins as seen by mass spectrometry

Volcano plots were created based on the MS data in order to visually identify the most dysregulated proteins between two conditions (Figure 2). With the threshold parameters used (z-score ≥ or ≤ 1.96; p-values and q-values ≤ 0.05), we found that HIV-1 vector infection alone and GS-CA1 treatment alone had little impact on nuclear envelope proteins, as previously observed in the PCA (Supplementary Figure S2). HIV-1 ($NL43_{GFP}$) infection resulted in the reduced relative abundance of only 5 proteins, *i.e.* Lysozyme C (LYZ), pH domain leucine-rich repeat-containing

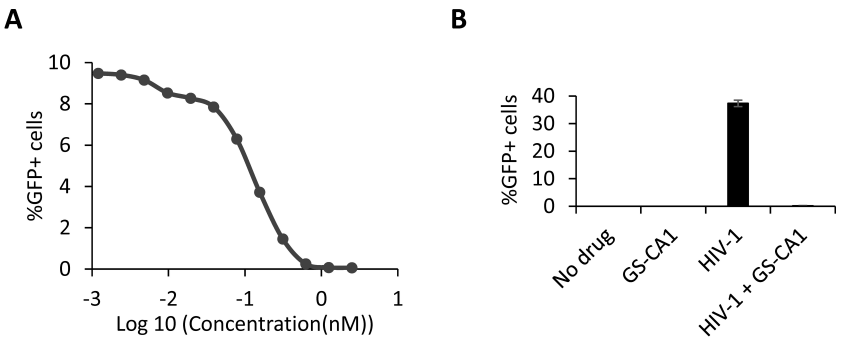

FIGURE 1
GS-CA1 efficiently inhibits HIV-1 early infection stages in THP-1 cells. **(A)** Dose-dependent inhibition of $NL43_{GFP}$. THP-1 cells were treated with multiple dilutions of GS-CA1 and infected with $NL43_{GFP}$ for 48 h, at which point, % GFP-positive cells were determined by FACS. **(B)** Infection control in mass spectrometry (MS) experiments. Cells were infected or not with $NL43_{GFP}$ (CRFK MOI = 2) and treated or not with 2 nM GS-CA1. 12 h later, cells were processed for MS but small aliquots were placed back in culture for one more day. % GFP-positive cells were determined by FACS. Shown are average data from 5 replicates, with standard deviations.

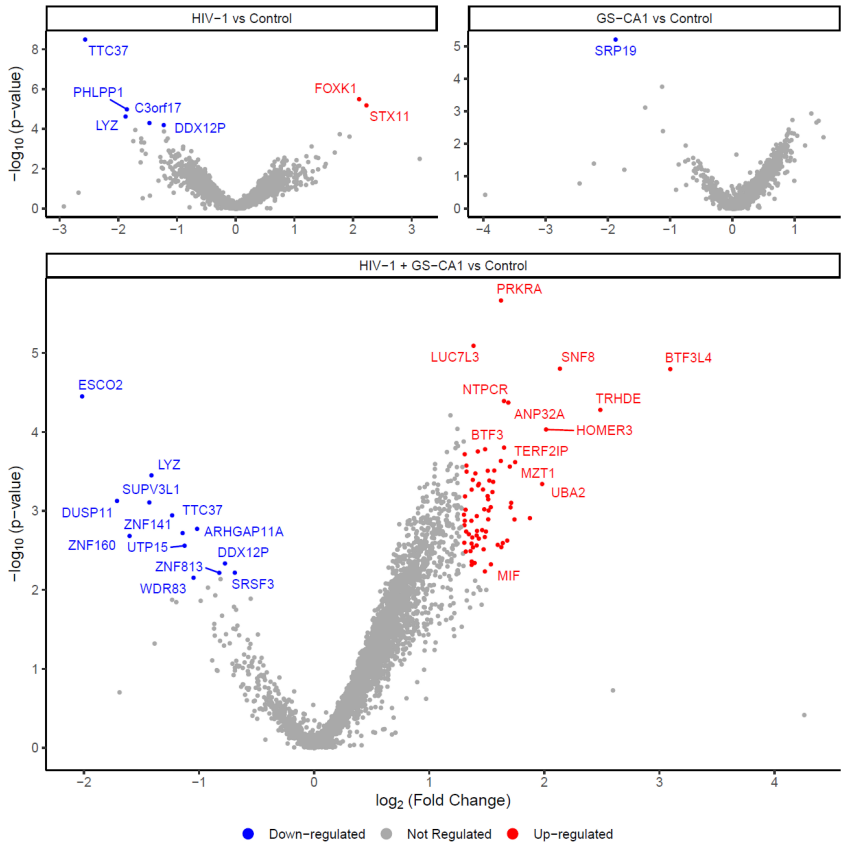

FIGURE 2
Modulation of proteins in nuclear envelope-enriched fractions by HIV-1 infection and GS-CA1 treatment. THP-1 cells were infected or not with $NL43_{GFP}$ (CRFK MOI = 2) and treated or not with 2 nM GS-CA1. Infections were done in quintuplicates. 12 h later, cells were processed for MS. Volcano plots show dysregulated proteins for $NL43_{GFP}$-infected cells compared to control (uninfected) cells (top left), GS-CA1-treated cells compared to control (untreated) cells (top right) and $NL43_{GFP}$-infected, GS-CA1-treated cells compared to control (uninfected, untreated) cells (bottom). Colored dots indicate proteins upregulated (red) or downregulated (blue). Grey dots indicate non-dysregulated proteins.

protein phosphatase 1 (PHLPP1), NEPRO (Nucleolus and neural progenitor protein; C3orf17), DEAD/H-box helicase 12 pseudogene (DDX12P) and tetratricopeptide repeat protein 37 (TTC37). The abundance of two proteins was increased by HIV-1 infection, *i.e.* forkhead box protein K1 (FOXK1) and Syntaxin-11 (STX11). Treatment with GS-CA1 led to the downregulation of only one cellular protein, signal recognition particle 19 (SRP19). Of note, none of the proteins found to be regulated by HIV-1 or GS-CA1 is known as an integral protein of the nuclear envelope, raising the possibility that they are transiently associating with the nuclear envelope. In contrast, HIV-1 infection in the presence of GS-CA1 altered the levels of 84 proteins, with 71 upregulated and 13 downregulated proteins. A full list of proteins regulated by HIV-1 and/or GS-CA1 is made available (see Supplementary Material). Again, most of these 84 proteins are not known as permanent nuclear envelope residents. Interestingly, several of them are interferon-stimulated gene products, according to the Interferome database (32). We also performed single-variable comparisons, i.e. HIV-1 + GS-CA1 vs HIV-1 and HIV-1 + GS-CA1 vs GS-CA1 (Supplementary Figure S4), and interestingly, we observed that HIV-1 was a much greater inducer of variation than GS-CA1 treatment.

Finally, in order to ascertain that the mass spectrometry approach chosen can detect an expected modulation pattern, we also treated THP-1 cells with IFN-β and then analyzed nuclear envelope-enriched fractions from treated and untreated cells (Supplementary Figure S5). Results showed that nearly 120 proteins were either downregulated or upregulated. As expected, most upregulated proteins were ISGs, including known antiviral factors such as Mx2 and ISG15 (33, 34). Interestingly, when we compared the proteins regulated by HIV-1 or HIV-1 + GS-CA1 treatment, on one hand, to the proteins regulated by IFN-I treatment, on the other hand, we found that SH3 domain-binding glutamic acid-rich-like protein 3 (SH3BGRL3) was upregulated in both conditions.

IFN-β but not GS-CA1 causes the accumulation of HIV-1 at the nuclear envelope

GS-CA1 was proposed to induce a block to nuclear import, though this is still disputed. Thus, we analyzed the presence in the nuclear envelope-enriched fractions of HIV-1 proteins-derived

peptides, which were not included in the results shown in Figure 2. We performed an identical analysis in cells treated or not with IFN-β, as this drug promotes the expression of ISGs, including Mx2 which was proposed to interfere with HIV-1 nuclear import by binding CA proteins (14). All the peptides detected were from the structural proteins matrix (MA) and capsid (CA). GS-CA1 did not result in any noticeable modulation in the relative abundance of these peptides in $NL43_{GFP}$-infected cells (Figure 3A). Remarkably, in the presence of IFN-β, a substantial increase in several of the HIV-1 peptides in the nuclear envelope extracts was evident (Figure 3B).

HIV-1 colocalizes with TPR in the presence of GS-CA1

To evaluate the impact of GS-CA1 on HIV-1 cellular distribution in the early stages of the infection, we conducted immunofluorescence microscopy experiments, staining for HIV-1 CA as well as the Nup TPR as a nucleopore marker. As shown Figure 4A, HIV-1 CA signal was present mostly as small "dots" which were found throughout the cells in the conditions used. Based on previous work from our team and others, those dots are expected to represent mostly individual HIV-1 cores/replication complexes (30, 35, 36). TPR was found almost entirely at the nuclear envelope and was partially found in the form of punctate signal consistent with NPCs. In a blinded analysis, we quantified the percentage of CA "dots" colocalizing with TPR, in absence or presence of GS-CA1 and IFN-β. Colocalization was rare, but examples are shown by white arrows in Figure 4A, whereas the quantification analysis is shown in Figure 4B. We found that in the presence of GS-CA1, the relative number of HIV-1 CA signal colocalizing with TPR increased by about 8-fold. Treatment with IFN-β also resulted in an increase in CA-TPR colocalization, but this phenotype was smaller compared with GS-CA1 (Figure 4B). However, IFN-β induced a distinct CA distribution, *i.e.* its accumulation in the immediate vicinity of the nuclear envelope, but not particularly at TPR-positive nuclear pore (see blue arrows in Figure 4A).

Discussion

The mechanisms of action for GS-6207 and related antiviral compounds need to be established more thoroughly. When this

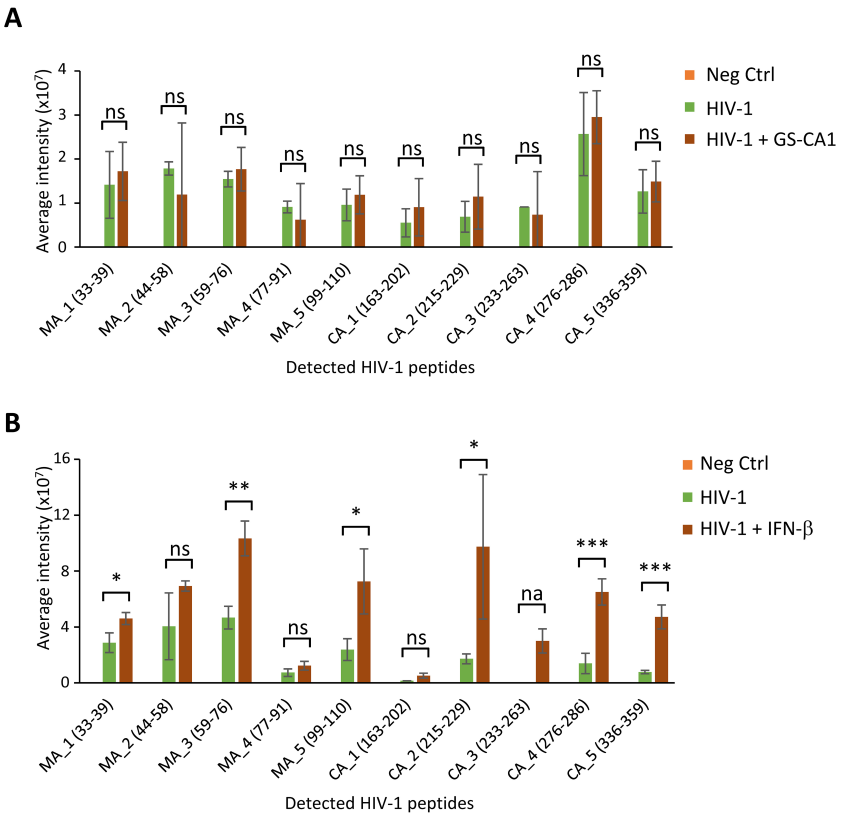

FIGURE 3
HIV-1 protein levels in nuclear envelope fractions are modulated by IFN-β but not GS-CA1. **(A)** Intensity of HIV-1 protein-associated peptides detected by MS in nuclear envelope-enriched fractions following infection with the $NL43_{GFP}$ vector in absence or presence of GS-CA1 (2nM), or in uninfected, untreated cells as a control (Neg Ctrl). Bars represent the average values from 5 replicates, with standard deviations. **(B)** Intensity of HIV-1 peptides in nuclear envelope-enriched fractions from cells infected with $NL43_{GFP}$ and treated or not with IFN-β (10 ng/ml) or in uninfected, untreated cells as a control (Neg Ctrl). Bars represent the average values from 3 replicates, with standard deviations. In both **(A, B)**, only peptides with intensity levels significantly above background were included. Statistical significance was determined using the one-tailed t-test. *$p < 0.05$; **$p < 0.005$; ***$p < 0.0005$; ns, not significant; na, not applicable due to a lack of detectable peptide in absence of GS-CA1.

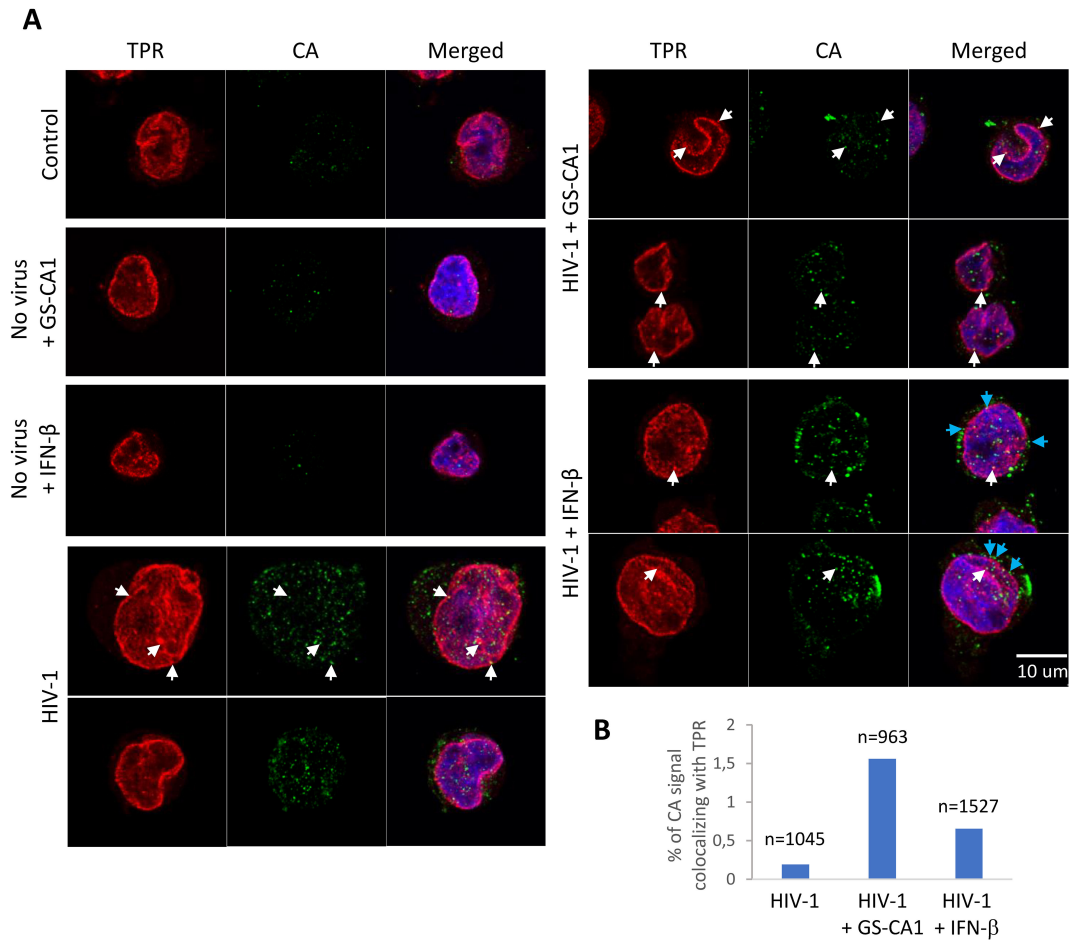

FIGURE 4
Effect of GS-CA1 and IFN-β on HIV-1 subcellular distribution. **(A)** THP-1 cells were infected with $NL43_{GFP}$ (CRFK MOI = 2) for 12 h in the presence or absence of either IFN-β added 12 h before infection) or GS-CA1 (added 2 h prior to infection). Cells were then fixed and stained with a CA antibody (green) and a TPR antibody (red). Hoechst 33342 was used to reveal DNA (blue). White arrows show examples of the CA-TPR colocalization whereas cyan arrows point to examples of CA signal accumulating in the vicinity of the nuclear envelope. **(B)** 20 randomly selected fields for each condition were used to count the percentage of CA signal "dots" colocalizing with TPR, relative to the total number of CA signal dots (see Methods). The total number of CA dots analyzed is shown on top of each bar.

project was initiated, GS-6207 was not approved yet, and the compound was not made available to us, but GS-CA1 was. We focused on the effect of GS-CA1 on HIV-1 functional interactions with the nuclear envelope. Mass spectrometry on nuclear envelope-enriched fractions had been done in the context of late stages of HIV-1 replication (37). To the best of our knowledge, no similar investigation had been conducted focusing on the early stages of the infection. We found that few proteins were modulated by either HIV-1 infection or GS-CA1 treatment alone (Figure 2), though of course, a different conclusion may be reached by using less stringent threshold parameters. Although SRP19 (downmodulated by GS-CA1) has been linked to the antiviral effect of APOBEC3G (38), none of the proteins found to be modulated are known to be involved in the early stages of HIV-1, and none are *bona fide* NPC components. The results obtained were strikingly different in cells that were both infected and GS-CA1-treated, since we found 71 upregulated and 13 downregulated proteins, upon comparison with the control cells (Figure 2). It is unlikely that the difference in phenotype between, on one hand, HIV-1 alone or GS-CA1 alone, and on the other hand, the HIV-1 + GS-CA1 combination, is due to cytotoxicity. The concentration of GS-CA1 used in this experiment, 2 nM, is well below the cytotoxic concentrations for this drug [CC50 > 30 μM (18)]. Also, less than half of the cells were infected in the control without drug in this experiment (Figure 1B), making it unlikely that the dose of virus used would have cytotoxic effects after 16 h of infection. Thus, we conclude that the modulation of nuclear envelope proteins in these conditions stems from the inhibition of the virus by GS-CA1. One possibility is that GS-CA1 causes HIV-1 cores to be sequestered at nuclear pores, leading to the increased presence of proteins interacting with them and/or proteins that are specialized sensors of viral pathogens. Along these lines, we found that SH3BGRL3, an IFN-β-stimulated protein in these cells, was also upregulated by HIV-1. Though no functional interactions between HIV-1 and SH3BGRL3 have been described so far, the

latter may be part of an antiviral response targeting the former. Another possibility is that HIV-1 may obstruct nuclear pores, leading to an accumulation of HIV-1-irrelevant proteins that normally transit through these pores. However, we did not observe modulation of Nups. It should be reminded that the HIV-1 vector used in this study was VSV-G-pseudotyped; the possibility that this affects the results obtained cannot be excluded.

Using MS, we were able to detect the presence of HIV-1 peptides in nuclear envelope-enriched fractions (Figure 3). Interestingly, all of the peptides that could be quantified belonged to MA or CA. Early work had involved MA as important for HIV-1 nuclear import, due to the presence of nuclear localization signals in this protein (39). Accordingly, MA was found long ago to co-purify with HIV-1 complexes present in the nucleus of acutely infected cells (40, 41). As stated in the introduction, the modern view of HIV-1 nuclear import is that an intact or nearly intact capsid core transits through the NPCs, which implies that MA proteins are totally dissociated from the HIV-1 complex that gains access to the nucleus; perhaps this new model over-simplifies HIV-1 nuclear import. HIV-1 MA and CA peptides were present in significantly higher amounts in nuclear envelope fractions in the presence of IFN-β. This effect might be explained by the IFN-induced overexpression of Mx2, a well-investigated host factor that stabilizes HIV-1 cores and inhibits their nuclear import (14). Upon immunofluorescence analysis of acutely infected cells (Figure 4), we did observe an increase in the relative colocalization of HIV-1 cores (as detected with a CA antibody) and NPCs stained with a TPR antibody, in presence of IFN-β. However, a more striking phenotype associated with IFN-β treatment was the accumulation of apparent HIV-1 capsid cores in close vicinity to the nucleus without a strong pattern of colocalization with TPR. By contrast, GS-CA1 caused a more pronounced phenotype of association with NPCs. Why, then, did we not see an increase in the relative amounts of HIV-1 peptides in nuclear envelope fractions upon GS-CA1 treatment (Figure 3)? A simple explanation is that even in the presence of the drug, we only detected a small fraction of total cellular CA signal as colocalizing with TPR in the microscopy experiment (1.5%), and thus modulation of this specifically NPC-associated population probably could not have been detected in the nuclear envelope-enriched fractions that were used for MS.

Taken together, our MS and microscopy data suggest that GS-CA1 causes a block to nuclear import in THP-1 cells by sequestration of HIV-1 capsid cores at nuclear pores, whereas IFN-β causes their retention at the nuclear envelope or in an as-yet-undefined cellular compartment that associates and co-purifies with the nuclear envelope. In addition, GS-CA1 causes the dysregulation of nuclear envelope fraction proteins in acutely HIV-1-infected cells, an effect that is not predicted by the analysis of drug toxicity in the absence of viral infection. Limitations to this study, however, include (i) the focus on a single monocytic cell line and the absence of data from cells of the lymphoid lineage; (ii) the use of VSV-G pseudotyping, as mentioned before; (iii) the use of a single inhibitor concentration and a single MOI. Future studies will need to include a more diverse set of conditions in order to more fully characterize the relevance of nuclear membranes to the mechanism of action of GS-CA1 or IFN-I.

Data availability statement

The original contributions presented in the study are included in the article/Supplementary Material and were previously uploaded here: https://figshare.com/projects/Singh_et_al_2025/194951. Further inquiries can be directed to the corresponding author/s.

Ethics statement

Ethical approval was not required for the studies on humans in accordance with the local legislation and institutional requirements because only commercially available established cell lines were used.

Author contributions

AS: Formal analysis, Investigation, Methodology, Visualization, Writing – original draft. VF: Formal analysis, Investigation, Methodology, Visualization, Writing – original draft. KS: Formal analysis, Methodology, Visualization, Writing – review & editing. HC: Investigation, Methodology, Writing – original draft. NM: Supervision, Writing – review & editing. AD: Funding acquisition, Resources, Supervision, Writing – review & editing. HG: Conceptualization, Funding acquisition, Supervision, Writing – review & editing. LB: Conceptualization, Formal analysis, Funding acquisition, Methodology, Project administration, Supervision, Writing – original draft, Writing – review & editing.

Funding

The author(s) declare that financial support was received for the research, authorship, and/or publication of this article. This study was funded by a grant (30-117) from the Canadian Foundation for AIDS Research (CANFAR) to LB, as well as a Queen Elizabeth Scholarship to AS, and FRQNT and MITACS Globalink Scholarships to KS.

Conflict of interest

The authors declare that the research was conducted in the absence of any commercial or financial relationships that could be construed as a potential conflict of interest.

The author(s) declared that they were an editorial board member of Frontiers, at the time of submission. This had no impact on the peer review process and the final decision.

Generative AI statement

The author(s) declare that no Generative AI was used in the creation of this manuscript.

Publisher's note

All claims expressed in this article are solely those of the authors and do not necessarily represent those of their affiliated organizations, or those of the publisher, the editors and the reviewers. Any product that may be evaluated in this article, or claim that may be made by its manufacturer, is not guaranteed or endorsed by the publisher.

Supplementary material

The Supplementary Material for this article can be found online at: https://www.frontiersin.org/articles/10.3389/fviro.2025.1547176/full#supplementary-material

References

1. Forshey BM, Von Schwedler U, Sundquist WI, Aiken C. Formation of a human immunodeficiency virus type 1 core of optimal stability is crucial for viral replication. *J Virol*. (2002) 76:5667–77. doi: 10.1128/JVI.76.11.5667-5677.2002

2. Lee K, Ambrose Z, Martin TD, Oztop I, Mulky A, Julias JG, et al. Flexible use of nuclear import pathways by HIV-1. *Cell Host Microbe*. (2010) 7:221–33. doi: 10.1016/j.chom.2010.02.007

3. Malikov V, Da Silva ES, Jovasevic V, Bennett G, De Souza Aranha Vieira DA, Schulte B, et al. HIV-1 capsids bind and exploit the kinesin-1 adaptor FEZ1 for inward movement to the nucleus. *Nat Commun*. (2015) 6:6660. doi: 10.1038/ncomms7660

4. Carnes SK, Zhou J, Aiken C. HIV-1 engages a dynein-dynactin-BICD2 complex for infection and transport to the nucleus. *J Virol*. (2018) 92. doi: 10.1128/JVI.00358-18

5. Engelman AN. HIV capsid and integration targeting. *Viruses*. (2021) 13. doi: 10.3390/v13010125

6. Petrovic S, Mobbs GW, Bley CJ, Nie S, Patke A, Hoelz A. Structure and function of the nuclear pore complex. *Cold Spring Harb Perspect Biol*. (2022) 14. doi: 10.1101/cshperspect.a041264

7. Aramburu IV, Lemke EA. Floppy but not sloppy: Interaction mechanism of FG-nucleoporins and nuclear transport receptors. *Semin Cell Dev Biol*. (2017) 68:34–41. doi: 10.1016/j.semcdb.2017.06.026

8. Schaller T, Ocwieja KE, Rasaiyaah J, Price AJ, Brady TL, Roth SL, et al. HIV-1 capsid-cyclophilin interactions determine nuclear import pathway, integration targeting and replication efficiency. *PloS Pathog*. (2011) 7:e1002439. doi: 10.1371/journal.ppat.1002439

9. Matreyek KA, Yucel SS, Li X, Engelman A. Nucleoporin NUP153 phenylalanine-glycine motifs engage a common binding pocket within the HIV-1 capsid protein to mediate lentiviral infectivity. *PloS Pathog*. (2013) 9:e1003693. doi: 10.1371/journal.ppat.1003693

10. Xue G, Yu HJ, Buffone C, Huang SW, Lee K, Goh SL, et al. The HIV-1 capsid core is an opportunistic nuclear import receptor. *Nat Commun*. (2023) 14:3782. doi: 10.1038/s41467-023-39146-5

11. Muller TG, Zila V, Muller B, Krausslich HG. Nuclear capsid uncoating and reverse transcription of HIV-1. *Annu Rev Virol*. (2022) 9:261–84. doi: 10.1146/annurev-virology-020922-110929

12. Dharan A, Talley S, Tripathi A, Mamede JI, Majetschak M, Hope TJ, et al. KIF5B and nup358 cooperatively mediate the nuclear import of HIV-1 during infection. *PloS Pathog*. (2016) 12:e1005700. doi: 10.1371/journal.ppat.1005700

13. Dharan A, Bachmann N, Talley S, Zwikelmaier V, Campbell EM. Nuclear pore blockade reveals that HIV-1 completes reverse transcription and uncoating in the nucleus. *Nat Microbiol*. (2020) 5:1088–95. doi: 10.1038/s41564-020-0735-8

14. Dicks MDJ, Betancor G, Jimenez-Guardeno JM, Pessel-Vivares L, Apolonia L, Goujon C, et al. Multiple components of the nuclear pore complex interact with the amino-terminus of MX2 to facilitate HIV-1 restriction. *PloS Pathog*. (2018) 14:e1007408. doi: 10.1371/journal.ppat.1007408

15. Merindol N, Berthoux L. Restriction factors in HIV-1 disease progression. *Curr HIV Res*. (2015) 13:448–61. doi: 10.2174/1570162X13666150608104412

16. Zhuang S, Torbett BE. Interactions of HIV-1 capsid with host factors and their implications for developing novel therapeutics. *Viruses*. (2021) 13. doi: 10.3390/v13030417

17. Shen Q, Wang YE, Palazzo AF. Crosstalk between nucleocytoplasmic trafficking and the innate immune response to viral infection. *J Biol Chem*. (2021) 297:100856. doi: 10.1016/j.jbc.2021.100856

18. Yant SR, Mulato A, Hansen D, Tse WC, Niedziela-Majka A, Zhang JR, et al. A highly potent long-acting small-molecule HIV-1 capsid inhibitor with efficacy in a humanized mouse model. *Nat Med*. (2019) 25:1377–84. doi: 10.1038/s41591-019-0560-x

19. Ogbuagu O, Segal-Maurer S, Ratanasuwan W, Avihingsanon A, Brinson C, Workowski K, et al. Efficacy and safety of the novel capsid inhibitor lenacapavir to treat multidrug-resistant HIV: week 52 results of a phase 2/3 trial. *Lancet HIV*. (2023) 10:e497–505. doi: 10.1016/S2352-3018(23)00113-3

20. Paik J. Lenacapavir: first approval. *Drugs*. (2022) 82:1499–504. doi: 10.1007/s40265-022-01786-0

21. Vidal SJ, Bekerman E, Hansen D, Lu B, Wang K, Mwangi J, et al. Long-acting capsid inhibitor protects macaques from repeat SHIV challenges. *Nature*. (2022) 601:612–6. doi: 10.1038/s41586-021-04279-4

22. Bester SM, Wei G, Zhao H, Adu-Ampratwum D, Iqbal N, Courouble VV, et al. Structural and mechanistic bases for a potent HIV-1 capsid inhibitor. *Science*. (2020) 370:360–4. doi: 10.1126/science.abb4808

23. Link JO, Rhee MS, Tse WC, Zheng J, Somoza JR, Rowe W, et al. Clinical targeting of HIV capsid protein with a long-acting small molecule. *Nature*. (2020) 584:614–8. doi: 10.1038/s41586-020-2443-1

24. Selyutina A, Hu P, Miller S, Simons LM, Yu HJ, Hultquist JF, et al. GS-CA1 and lenacapavir stabilize the HIV-1 core and modulate the core interaction with cellular factors. *iScience*. (2022) 25:103593. doi: 10.1016/j.isci.2021.103593

25. He J, Chen Y, Farzan M, Choe H, Ohagen A, Gartner S, et al. CCR3 and CCR5 are co-receptors for HIV-1 infection of microglia. *Nature*. (1997) 385:645–9. doi: 10.1038/385645a0

26. Merindol N, El-Far M, Sylla M, Masroori N, Dufour C, Li JX, et al. HIV-1 capsids from B27/B57+ elite controllers escape Mx2 but are targeted by TRIM5alpha, leading to the induction of an antiviral state. *PloS Pathog*. (2018) 14:e1007398. doi: 10.1371/journal.ppat.1007398

27. Masroori N, Cherry P, Merindol N, Li JX, Dufour C, Poulain L, et al. Gene knockout shows that PML (TRIM19) does not restrict the early stages of HIV-1 infection in human cell lines. *mSphere*. (2017) 2. doi: 10.1128/mSphereDirect.00233-17

28. Pawlica P, Dufour C, Berthoux L. Inhibition of microtubules and dynein rescues human immunodeficiency virus type 1 from owl monkey TRIMCyp-mediated restriction in a cellular context-specific fashion. *J Gen Virol*. (2015) 96:874–86. doi: 10.1099/jgv.0.000018

29. Kedzierska K, Crowe SM. The role of monocytes and macrophages in the pathogenesis of HIV-1 infection. *Curr Med Chem*. (2002) 9:1893–903. doi: 10.2174/0929867023368935

30. Mcdonald D, Vodicka MA, Lucero G, Svitkina TM, Borisy GG, Emerman M, et al. Visualization of the intracellular behavior of HIV in living cells. *J Cell Biol*. (2002) 159:441–52. doi: 10.1083/jcb.200203150

31. Davis LI, Blobel G. Nuclear pore complex contains a family of glycoproteins that includes p62: glycosylation through a previously unidentified cellular pathway. *Proc Natl Acad Sci U.S.A*. (1987) 84:7552–6. doi: 10.1073/pnas.84.21.7552

32. Rusinova I, Forster S, Yu S, Kannan A, Masse M, Cumming H, et al. Interferome v2.0: an updated database of annotated interferon-regulated genes. *Nucleic Acids Res*. (2013) 41:D1040–1046. doi: 10.1093/nar/gks1215

33. Morales DJ, Lenschow DJ. The antiviral activities of ISG15. *J Mol Biol*. (2013) 425:4995–5008. doi: 10.1016/j.jmb.2013.09.041

34. Betancor G, Jimenez-Guardeno JM, Lynham S, Antrobus R, Khan H, Sobala A, et al. MX2-mediated innate immunity against HIV-1 is regulated by serine phosphorylation. *Nat Microbiol*. (2021) 6:1031–42. doi: 10.1038/s41564-021-00937-5

35. Pawlica P, Berthoux L. Cytoplasmic dynein promotes HIV-1 uncoating. *Viruses*. (2014) 6:4195–211. doi: 10.3390/v6114195

36. Nepveu-Traversy ME, Demogines A, Fricke T, Plourde MB, Riopel K, Veillette M, et al. A putative SUMO interacting motif in the B30.2/SPRY domain of rhesus macaque TRIM5alpha important for NF-kappaB/AP-1 signaling and HIV-1 restriction. *Heliyon*. (2016) 2:e00056. doi: 10.1016/j.heliyon.2015.e00056

37. Monette A, Pante N, Mouland AJ. HIV-1 remodels the nuclear pore complex. *J Cell Biol*. (2011) 193:619–31. doi: 10.1083/jcb.201008064

38. Wang T, Tian C, Zhang W, Luo K, Sarkis PT, Yu L, et al. 7SL RNA mediates virion packaging of the antiviral cytidine deaminase APOBEC3G. *J Virol*. (2007) 81:13112–24. doi: 10.1128/JVI.00892-07

39. Haffar OK, Popov S, Dubrovsky L, Agostini I, Tang H, Pushkarsky T, et al. Two nuclear localization signals in the HIV-1 matrix protein regulate nuclear import of the HIV-1 pre-integration complex. *J Mol Biol*. (2000) 299:359–68. doi: 10.1006/jmbi.2000.3768

40. Bukrinsky MI, Sharova N, Mcdonald TL, Pushkarskaya T, Tarpley WG, Stevenson M. Association of integrase, matrix, and reverse transcriptase antigens of human immunodeficiency virus type 1 with viral nucleic acids following acute infection. *Proc Natl Acad Sci U.S.A*. (1993) 90:6125–9. doi: 10.1073/pnas.90.13.6125

41. Miller MD, Farnet CM, Bushman FD. Human immunodeficiency virus type 1 preintegration complexes: studies of organization and composition. *J Virol*. (1997) 71:5382–90. doi: 10.1128/jvi.71.7.5382-5390.1997